

Supporting Information for:

On the Use of NMR Distance Measurements for Assessing Surface Site Homogeneity

Frédéric A. Perras^{*a,b}, Damien B. Culver^a

^aChemical and Biological Sciences Division, Ames National Laboratory, Ames, IA 50011, USA

^bDepartment of Chemistry, Iowa State University, Ames, IA 50011, USA

*fperras@ameslab.gov

Synthetic procedures

General

All manipulations were performed under an inert atmosphere of nitrogen or argon on a Schlenk line or in a glovebox. THF- d_8 and benzene- d_6 were purchased from Cambridge Isotope Laboratories and dried over 3 Å molecular sieves prior to use. Pentane was purchased anhydrous from Sigma Aldrich and stored over activated 3 Å molecular sieves prior to use. Anhydrous methanol and tetrahydrofuran were purchased from Sigma Aldrich. Triethylamine was dried over CaH_2 , distilled under vacuum, and stored over 3 Å molecular sieves prior to use. High surface area γ -alumina ($\text{BET} = 250 \text{ m}^2 \text{ g}^{-1}$) was purchased from Fisher scientific in granule form, sieved to 400 – 250 μm , and dehydroxylated under high vacuum (10^{-5} torr) for 12 hours at 400, 600, 800, or 1000 °C following the previously outlined procedure.¹

^1H NMR spectra were recorded on a Varian MR-400 spectrometer ($^1\text{H} = 399.80 \text{ MHz}$). FTIR spectroscopic analyses were performed on a Bruker Alpha II spectrometer with a transmission module using self-supported 7 mm pellets within an argon filled glovebox. Methane quantifications were performed on an HP 6890 series GC system with an FID detector and an Agilent GS-GASPRO column. Zr analyses were performed on an Agilent 5800 ICP-OES spectrometer. ICP samples were prepared by soaking the solid samples (20 mg) in nitric acid (20 % v/v) overnight, followed by dilution to 2 % nitric acid.

General procedure for the grafting of $\text{Me}_2\text{SiCp}_2\text{ZrMe}_2$ on partially dehydroxylated alumina

In a Schlenk flask, partially dehydroxylated alumina (200 mg) was suspended in pentane (2 mL). While stirring (100 rpm), a solution of $\text{Me}_2\text{SiCp}_2\text{ZrMe}_2$ in pentane (34 mM, 2.5 mL, 0.085 mmol,) was added dropwise to the suspension. The reaction was stirred for 30 minutes, then the solution was removed by decantation and the solid was washed twice with pentane (5 mL each time). The solid was dried for 30 minutes under high vacuum, then stored under in an argon filled glovebox. FTIR spectra and Zr loading data are provided below. Methane formation was determined by loading partially dehydroxylated alumina (100 mg) and $\text{Me}_2\text{SiCp}_2\text{ZrMe}_2$ (13.1 mg, 0.043 mmol) into a round bottom flask (10 mL) and fitting it with a Schlenk adapter in an argon filled glovebox. On a high vacuum Schlenk line, pentane (2 mL) was vacuum distilled into the flask containing the solids at 77 K. The flask was sealed under static vacuum and stirred (100 rpm) for 30 minutes at room temperature. Afterwards, the volatiles were transferred via vacuum distillation to a 1 L flask with a Schlenk adapter at 77 K. The flask was allowed to warm up to room temperature and equilibrate until everything was in the gas phase then analyzed by GC-FID for methane content. A summary of the data is provided in Table S1.

Table S1. Summary of characterization data for the zirconocene grafted on activated alumina.

Dehydroxylation temp. (°C)	Color	Zr (% mass) ^a	Zr (mmol g ⁻¹) ^a	CH ₄ (mmol g ⁻¹) ^b	CH ₄ :Zr
400	beige	2.1 (3)	0.23 (3)	0.36 (4)	1.6 (2)
600	light yellow	2.4 (2)	0.27 (2)	0.32 (1)	1.20 (5)
800	light orange	1.6 (2)	0.18 (2)	0.14 (4)	0.8 (2)
1000	light pink	0.63 (3)	0.070 (3)	0.04 (2)	0.6 (2)

^aICP analyses were run in triplicate, standard deviations are given in parentheses. ^bMethane released measurements were performed in duplicate and the errors are given in the parentheses.

Attempts to synthesize the dimethoxy zirconocene precursor

Me₂SiCp₂ZrCl₂ + MeOH + Et₃N: In a PTFE valved NMR tube, Me₂SiCp₂ZrCl₂ (20 mg, 57 μmol) was suspended in THF-*d*₈ (0.5 mL) then MeOH in THF (5 % v/v, 0.10 mL, 0.13 mmol) and Et₃N (18 μL, 0.13 mol) were added to the NMR tube. The reaction was monitored by solution NMR spectroscopy (**Figure S12**). Within 3 hours most of the Me₂SiCp₂ZrCl₂ is consumed and several new species form, along with insoluble triethylammonium chloride. After heating at 75 °C for several days, other new species form based on the complicated Si(CH₃)₂ region, suggesting that the reaction results in multiple species and not the desired Me₂SiCp₂Zr(OMe)₂ complex with C_{2h} symmetry.

Me₂SiCp₂ZrMe₂ + MeOH: In a PTFE valved NMR tube, Me₂SiCp₂ZrMe₂ (20 mg, 65 μmol) was suspended in benzene-*d*₆ (0.5 mL) then MeOH in THF (5 % v/v, 0.11 mL, 0.14 mmol) was added by syringe. The reaction was shaken and monitored by solution NMR spectroscopy (**Figure S13**). After 30 minutes, all of the Me₂SiCp₂ZrMe₂ is consumed and a new species with C_s symmetry formed cleanly that is assigned to Me₂SiCp₂Zr(OMe)Me, along with methane was observed. Allowing the reaction to run for 3 hours resulted in the formation of several new signals due to the formation of several new species, not just the desired Me₂SiCp₂Zr(OMe)₂ complex.

Supplementary Figures

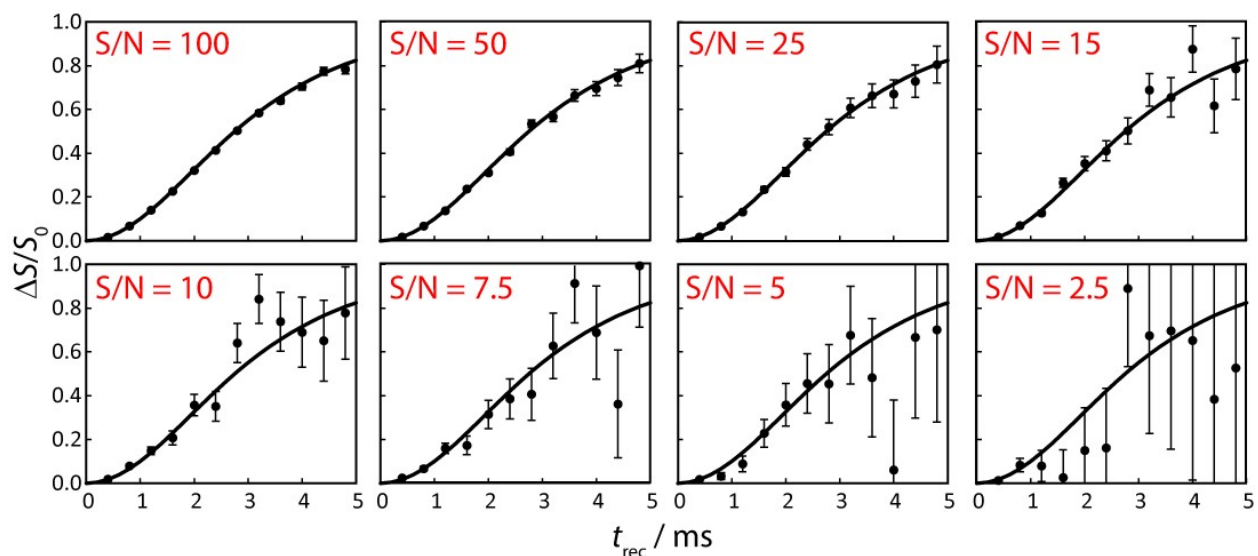


Figure S1. Example synthetic $^{13}\text{C}\{^{27}\text{Al}\}$ RESPDOR data with added Gaussian noise at different maximum S/N levels, with a T_2 of 5 ms. Error bars are presented as 1σ .

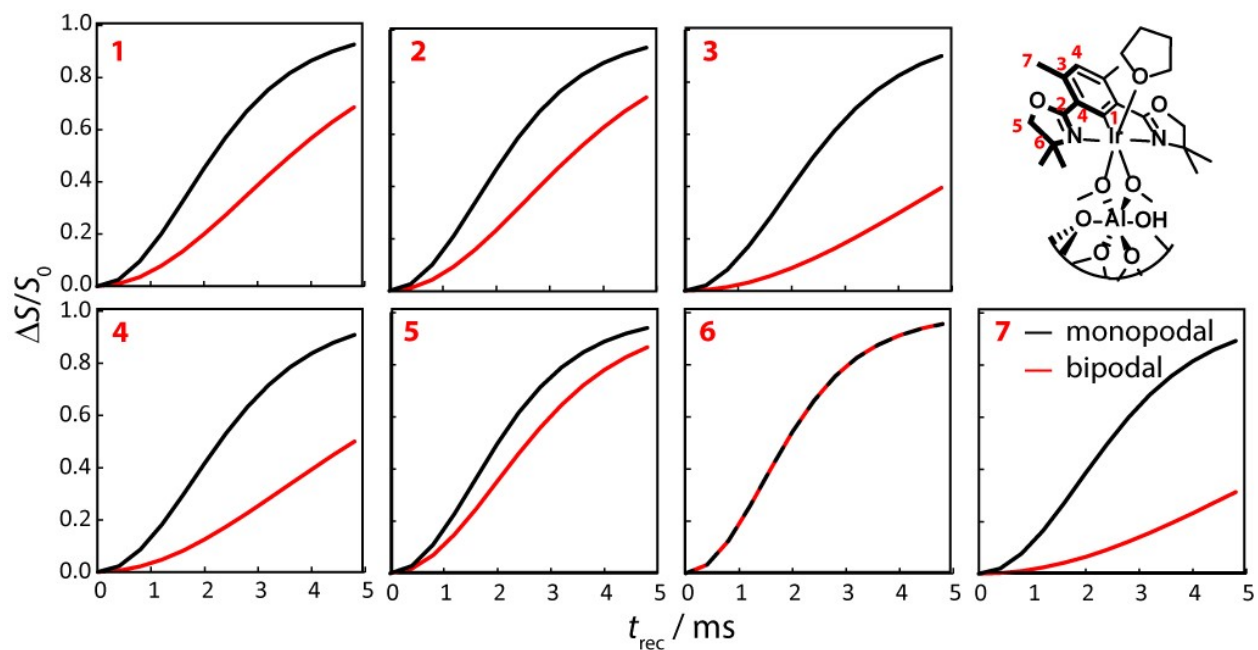


Figure S2. Synthetic $^{13}\text{C}\{^{27}\text{Al}\}$ surface-to-atom RESPDOR data for the pictured $(^{dm}\text{Phebox})\text{Ir}/\text{Al}_2\text{O}_3$. Two sets of simulated curves are shown for a more prone monopodal structure (black) and a bipodal configuration (red).

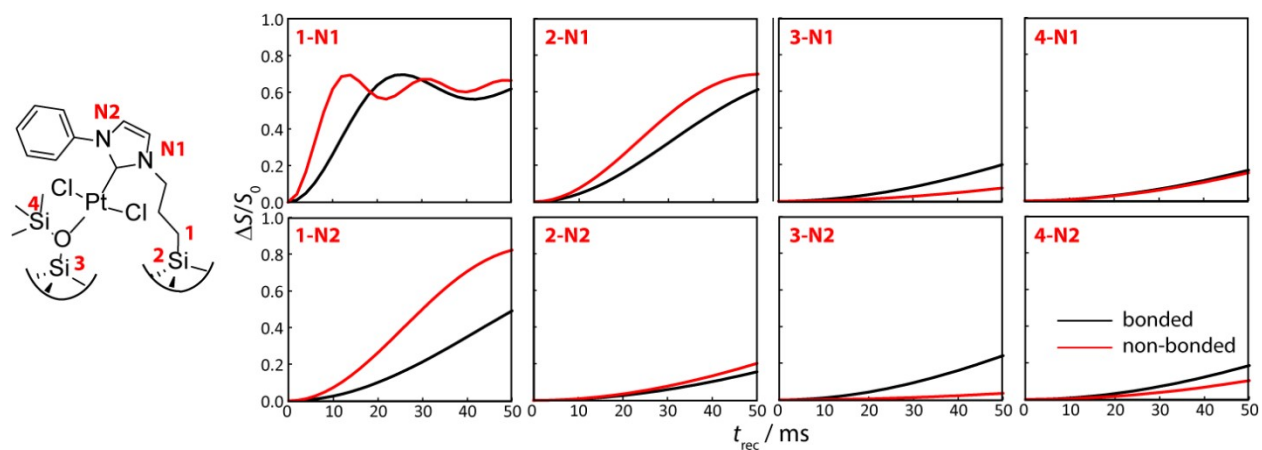


Figure S3. Synthetic $^{13}\text{C},^{29}\text{Si}\{^{15}\text{N}\}$ REDOR data for the pictured (NHC)Pt/SiO₂. Two sets of simulated curves are shown, one for a structure with a Pt-O-TMS interaction (black) and one without this interaction (red).

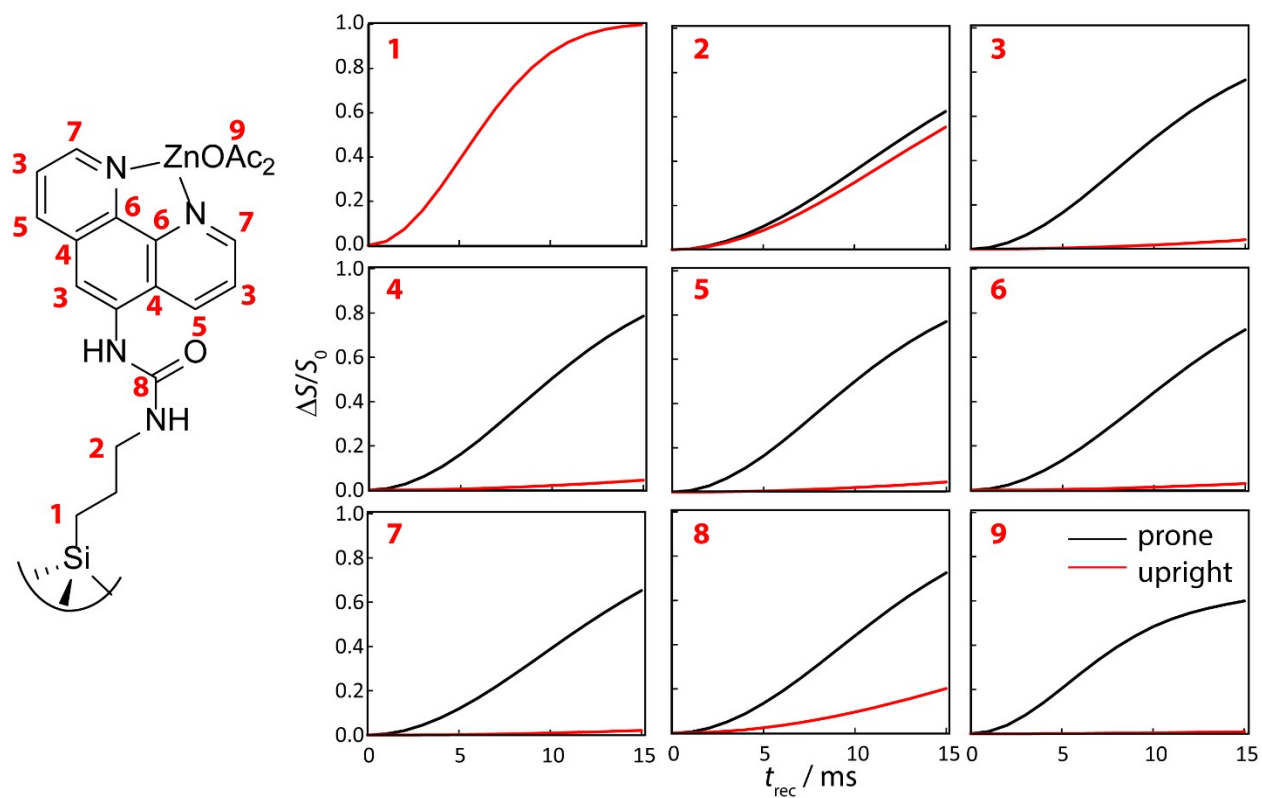


Figure S4. Synthetic $^{13}\text{C}\{^{29}\text{Si}\}$ REDOR data for the pictured (Phen)Zn/SiO₂. Two sets of simulated curves are shown, one for a structure with a prone structure (black) and one where the ligand is standing up from the surface (red).

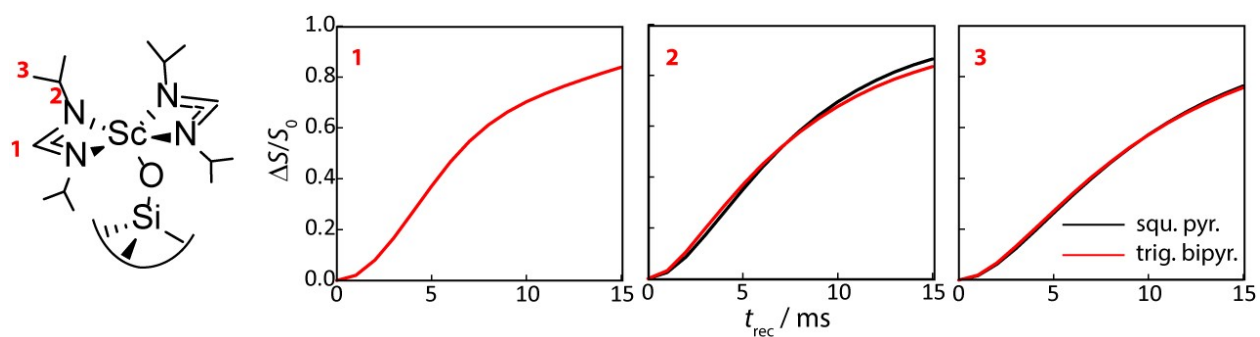


Figure S5. Synthetic $^{13}\text{C}\{^{29}\text{Si}\}$ REDOR data for the pictured $(\kappa^2\text{-(NiPr)}_2\text{CH})_2\text{Sc}/\text{SiO}_2$. Two sets of simulated curves are shown, one for a structure with a square pyramidal structure (black) and one with a trigonal bipyramidal structure (red).

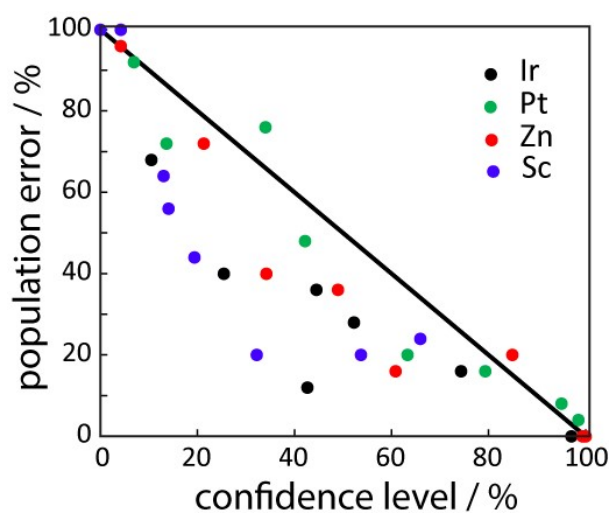


Figure S6. Correlation between the confidence level for the various 2-structure fits and the relative error in the predicted site populations. The black line corresponds to error=100%-confidence level.

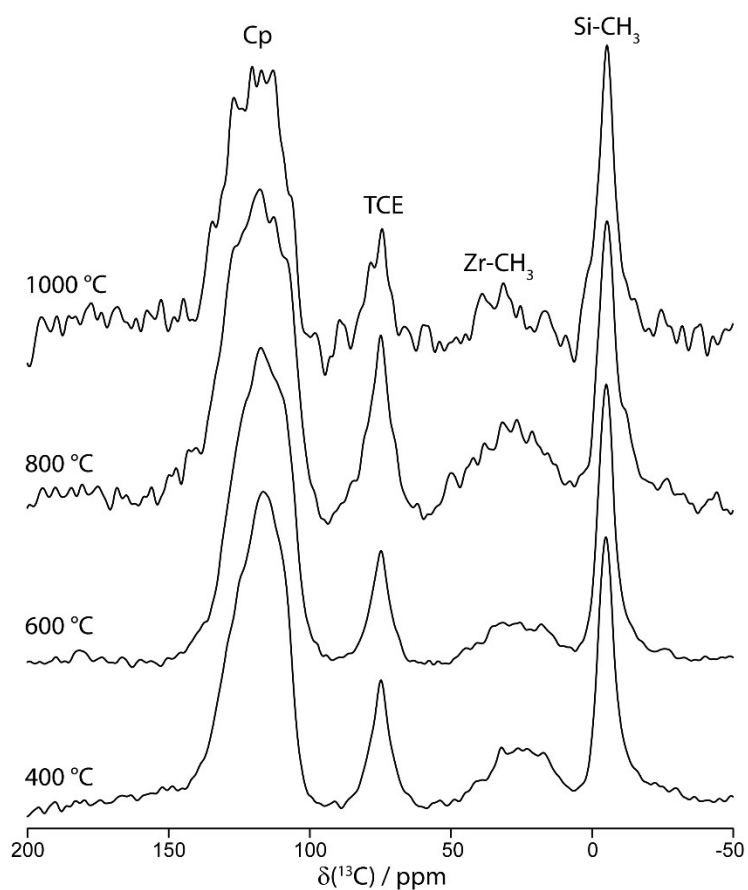


Figure S7. DNP-enhanced ^{13}C CPMAS NMR spectra acquired for the $\text{Zr}/\text{Al}_2\text{O}_3$ complexes grafted onto Al_2O_3 that was thermally activated at different temperatures, as indicated on the Figure.

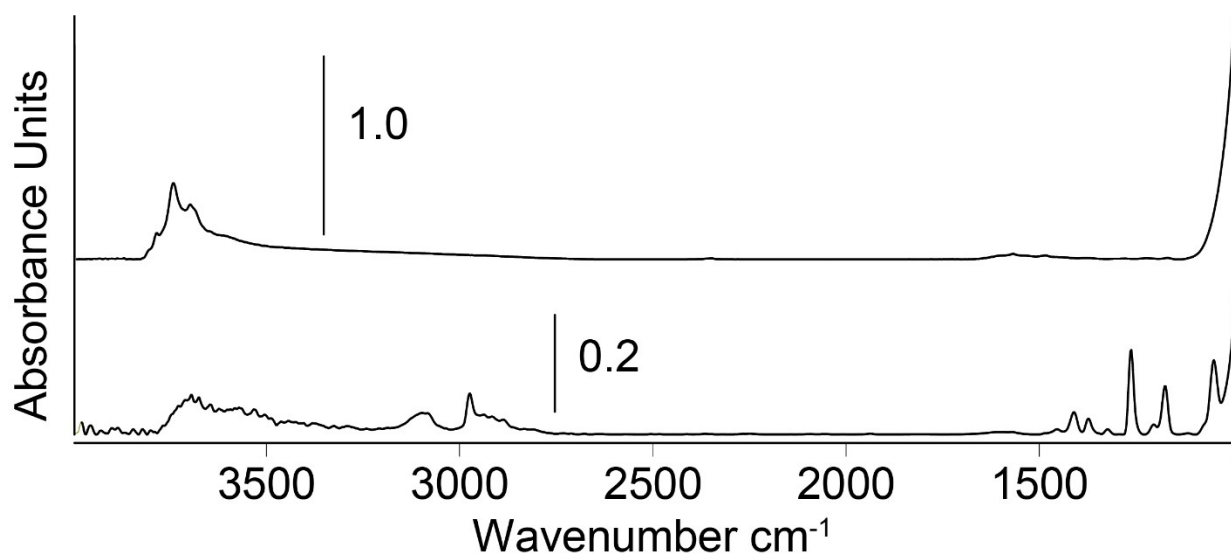


Figure S8. FTIR spectra of γ -alumina dehydroxylated at $400\text{ }^\circ\text{C}$ before (top) and after reaction with $\text{Me}_2\text{SiCp}_2\text{ZrMe}_2$ (bottom).

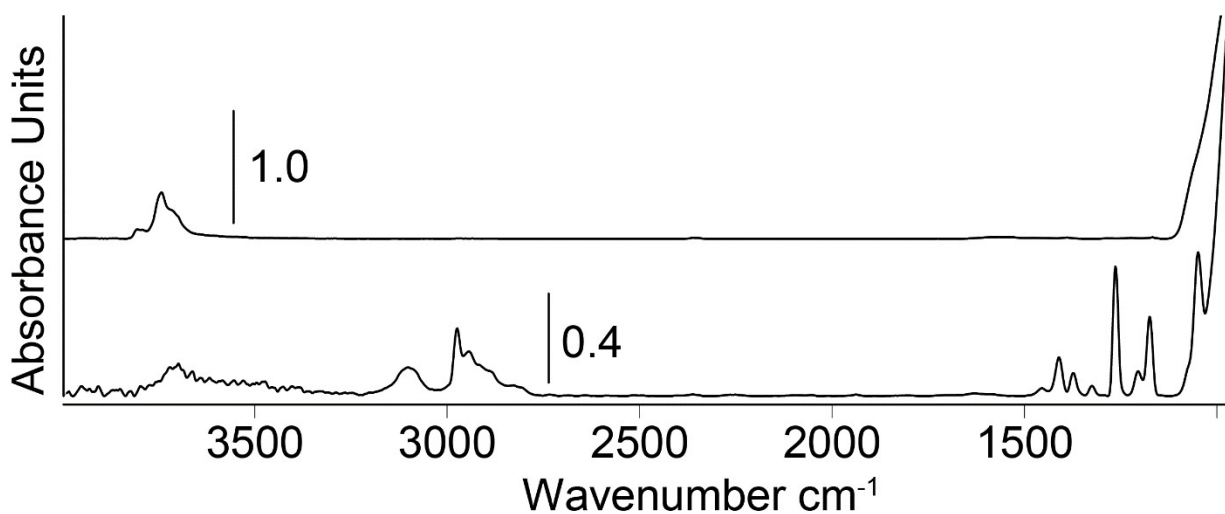


Figure S9. FTIR spectra of γ -alumina dehydroxylated at 600 °C before (top) and after reaction with Me₂SiCp₂ZrMe₂ (bottom).

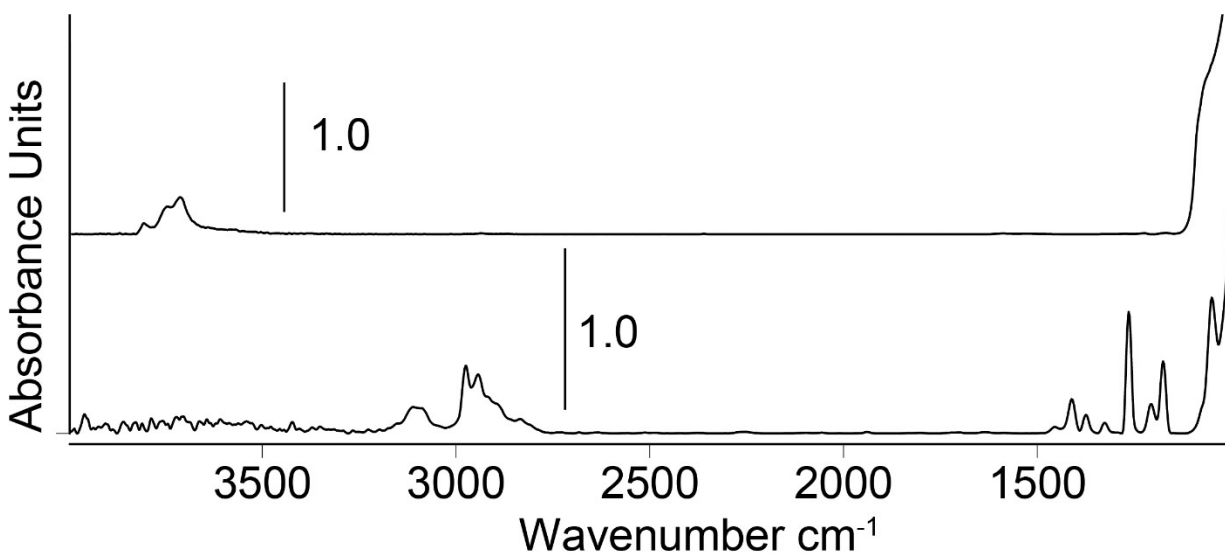


Figure S10. FTIR spectra of γ -alumina dehydroxylated at 800 °C before (top) and after reaction with Me₂SiCp₂ZrMe₂ (bottom).

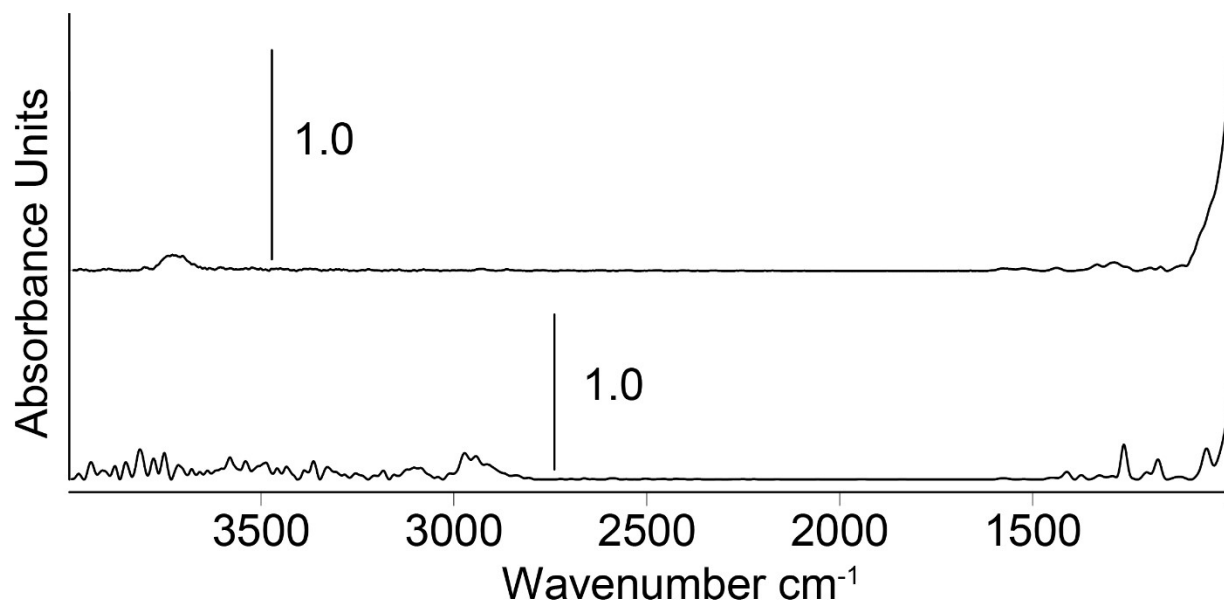


Figure S11. FTIR spectra of γ -alumina dehydroxylated at 1000 °C before (top) and after reaction with Me₂SiCp₂ZrMe₂ (bottom).

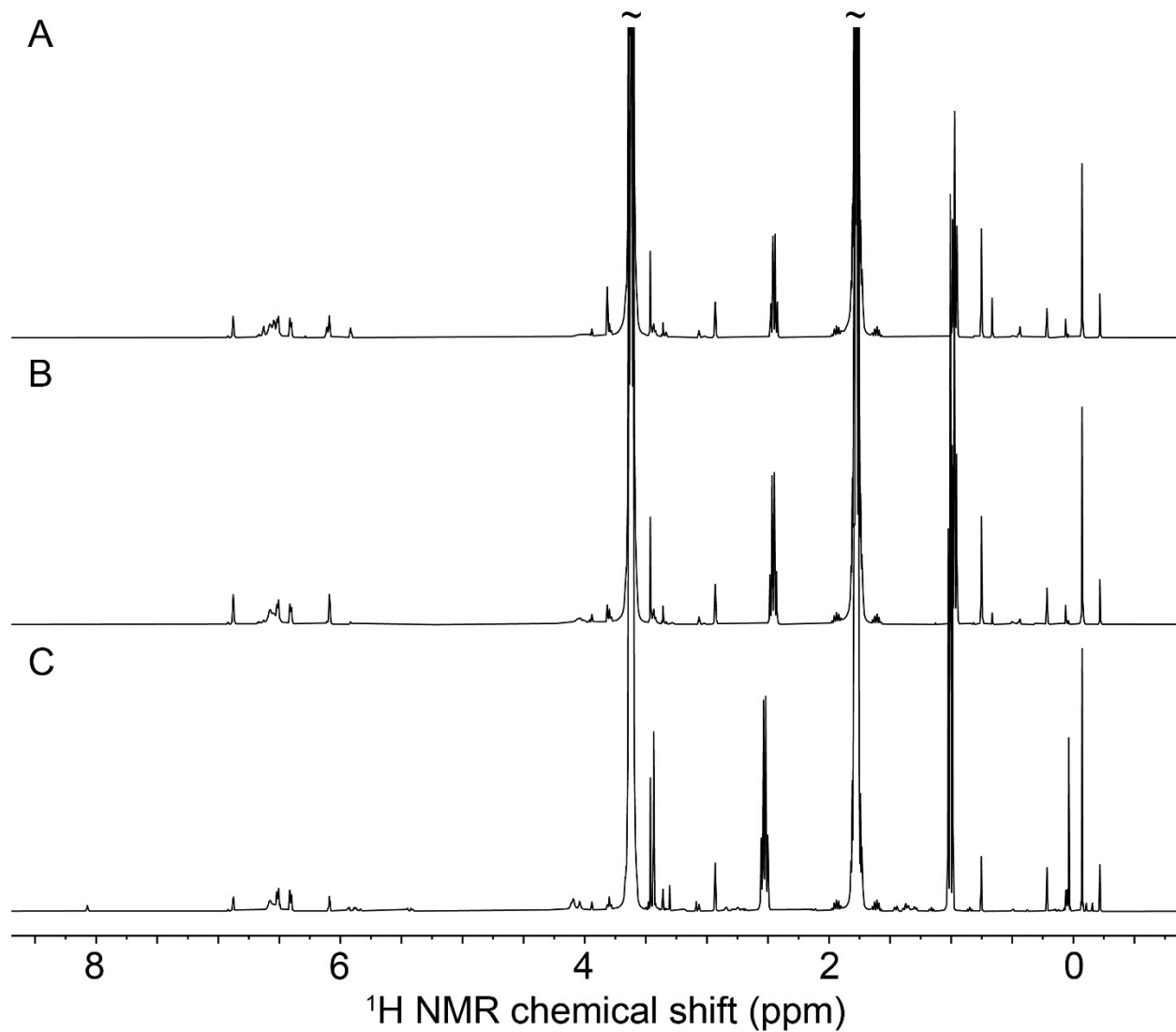


Figure S12. ^1H NMR spectra of the reaction of $\text{Me}_2\text{SiCp}_2\text{ZrCl}_2$ with MeOH and Et_3N in THF- d_8 after 3 hours at room temperature (A), 2 hours at 75 °C (B), and 3 days at 75 °C (C). ~ denotes THF signal cutoffs.

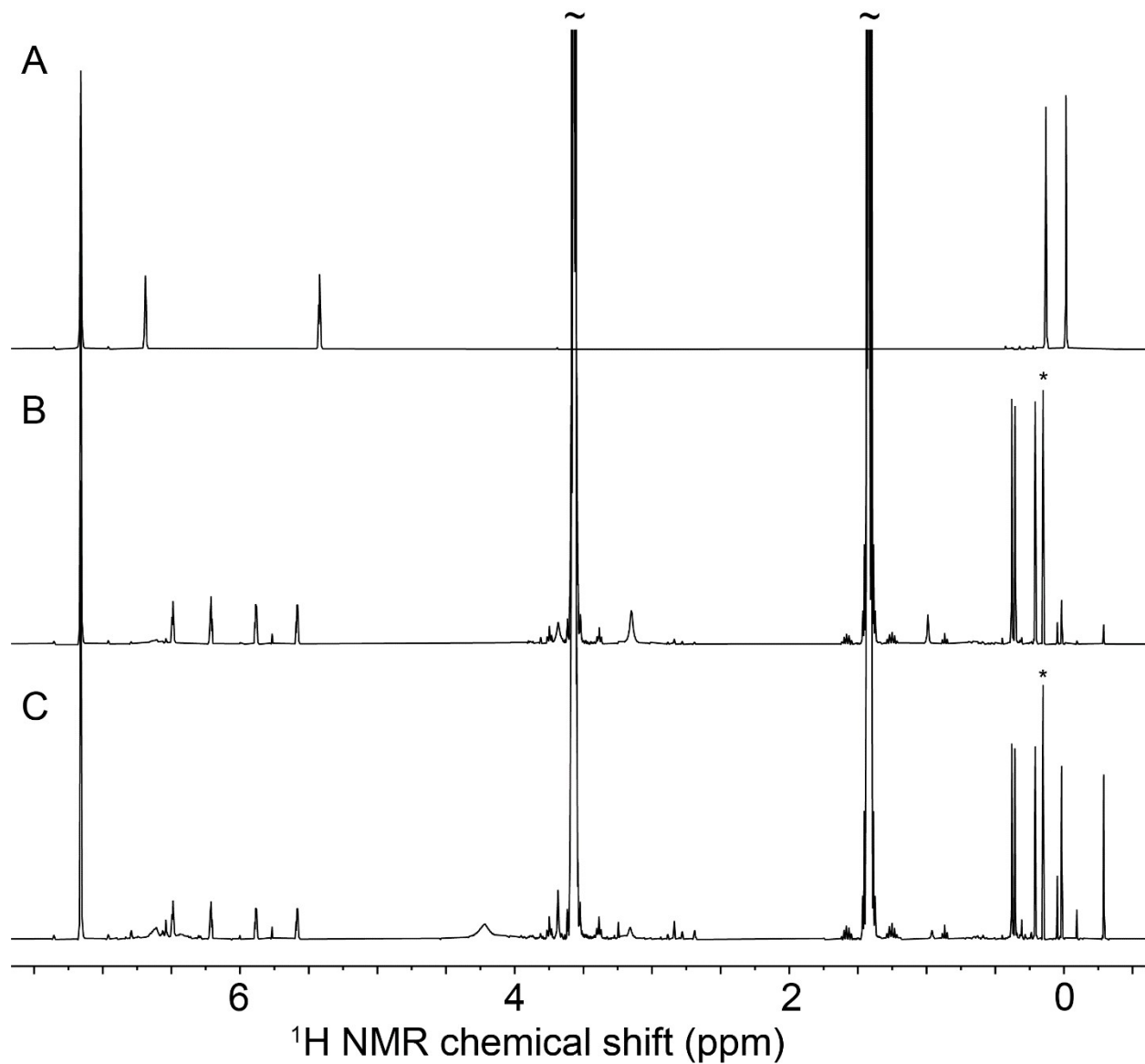


Figure S13. ^1H NMR spectra of the reaction of $\text{Me}_2\text{SiCp}_2\text{ZrMe}_2$ with MeOH in $\text{benzene-}d_6$ prior to addition (A), 30 minutes at room temperature after addition of MeOH (B), and 3 hours at room temperature after addition of MeOH (C). ~ denotes THF signal cutoffs. * denotes methane.

Supplementary Tables

Table S2. Quality and accuracy of fits to synthetic RESPDOR data for (*dm*Phebox)Ir/Al₂O₃ (50:50).

S/N	1-structure χ^2	2-structure χ^2	CL / %	structure accuracy / %	population deviation / %
100	0.4481	0.0332	100.0	100	0
	0.4566	0.0288			
	0.4593	0.0209			
	0.4728	0.0281			
	0.4915	0.0365			
	<0.4657>	<0.0295>			
50	0.5534	0.1147	97.1	100	0
	0.5403	0.0750			
	0.5921	0.0942			
	0.6086	0.1063			
	0.5591	0.0986			
	<0.5707>	<0.0978>			
25	1.1361	0.5100	74.3	90	16
	0.9364	0.4288			
	1.0782	0.3580			
	1.0325	0.4848			
	0.8737	0.4170			
	<1.0114>	<0.4397>			
15	1.9574	1.0209	52.3	100	28
	1.8258	1.2347			
	1.7593	1.1381			
	1.6744	1.2902			
	1.3297	0.9335			
	<1.7093>	<1.1235>			
10	4.2174	3.2931	42.6	80	12
	3.3696	2.7496			
	5.6838	4.1843			
	4.5922	3.2423			
	4.8218	3.6374			
	<4.5370>	<3.4213>			
7.5	4.7797	4.0539	44.5	60	36
	8.9076	6.0431			
	7.3497	5.2365			
	7.6114	5.7143			
	11.138	7.8920			
	<7.9575>	<5.7879>			
5	384.44	349.02	25.4	20	40
	34.619	23.957			
	32.917	23.376			
	49.985	49.857			
	93.921	93.908			
	<119.17>	<108.02>			
2.5	1106.3	1008.6	10.5	0	68
	63.462	61.540			
	80.018	80.018			
	74.876	74.810			
	78.805	77.183			
	<280.69>	<260.43>			

Table S3. Quality and accuracy of fits to synthetic RESPDOR data for (*dm*Phebox)Ir/Al₂O₃ (60:40).

S/N	1-structure χ^2	2-structure χ^2	CL / %	structure accuracy / %	population deviation / %
100	0.4465	0.0237	100.0	100	0
	0.4556	0.0188			
	0.4549	0.0277			
	0.4581	0.0254			
	0.4833	0.0240			
	<0.4597>	<0.0239>			
50	0.5646	0.1084	95.0	100	3
	0.5708	0.1215			
	0.5307	0.1278			
	0.6005	0.1076			
	0.5363	0.1103			
	<0.5606>	<0.1151>			
25	0.9910	0.4165	75.6	100	13
	1.0598	0.5049			
	1.1194	0.4301			
	0.9793	0.4309			
	0.8720	0.3490			
	<1.0043>	<0.4263>			
15	1.6982	0.9840	54.0	90	23
	1.4342	0.9771			
	1.4922	1.0859			
	1.4534	0.9321			
	2.4423	1.4704			
	<1.7041>	<1.0899>			
10	3.1743	2.3905	56.3	60	13
	3.1583	2.2109			
	6.6275	3.7552			
	8.0942	4.1265			
	5.1078	2.9691			
	<5.2324>	<3.0904>			
7.5	14.119	9.3228	47.1	60	13
	9.5851	6.8002			
	4.8512	4.0138			
	21.792	14.099			
	8.9573	6.5266			
	<11.861>	<8.1526>			
5	61.108	59.492	24.8	40	43
	22.861	16.406			
	15.225	13.274			
	365.34	365.32			
	26.878	22.602			
	<98.283>	<95.420>			
2.5	79.863	79.667	12.9	10	60
	82.961	82.954			
	66.735	66.675			
	54.419	49.993			
	61.236	51.254			
	<69.043>	<66.108>			

Table S4. Quality and accuracy of fits to synthetic RESPDOR data for (*dm*Phebox)Ir/Al₂O₃ (70:30).

S/N	1-structure χ^2	2-structure χ^2	CL / %	structure accuracy / %	population deviation / %
100	0.4820	0.0225	100.0	100	0
	0.5427	0.0303			
	0.5395	0.0266			
	0.5309	0.0303			
	0.5066	0.0254			
	<0.5203>	<0.0270>			
50	0.6132	0.1273	95.7	100	0
	0.6232	0.1169			
	0.5650	0.1021			
	0.7306	0.1335			
	0.5698	0.1245			
	<0.6204>	<0.1209>			
25	0.6994	0.2837	74.8	100	3
	0.9597	0.5042			
	1.0891	0.3421			
	1.0980	0.4360			
	0.7498	0.3873			
	<0.9192>	<0.3907>			
15	1.6298	1.1582	53.0	90	26
	2.2767	1.6042			
	1.8911	1.4206			
	1.5865	0.9442			
	2.1200	1.1033			
	<1.9008>	<1.2461>			
10	4.3201	2.4540	44.2	80	11
	3.6404	2.3380			
	2.9774	2.5391			
	2.6124	2.1031			
	5.9894	4.9798			
	<3.9079>	<2.8828>			
7.5	6.2504	4.8824	32.6	60	14
	5.1177	4.3074			
	50.246	49.268			
	4.7910	4.1924			
	13.431	9.4393			
	<15.967>	<14.418>			
5	252.86	246.93	24.4	30	43
	42.029	27.873			
	40.889	34.960			
	56.748	55.998			
	19.810	19.033			
	<82.469>	<76.959>			
2.5	122.86	122.86	0.7	0	43
	60.107	60.107			
	79.092	79.000			
	69.874	69.867			

78.352	78.352
<82.057>	<82.038>

Table S5. Quality and accuracy of fits to synthetic RESPDOR data for (*dm*Phebox)Ir/Al₂O₃ (80:20).

S/N	1-structure χ^2	2-structure χ^2	CL / %	structure accuracy / %	population deviation / %
100	0.4429	0.0225	100.0	100	0
	0.4378	0.0334			
	0.4783	0.0200			
	0.4865	0.0352			
	0.4621	0.0237			
	<0.4615>	<0.0270>			
50	0.5419	0.1055	94.6	100	0
	0.6087	0.1182			
	0.4733	0.0979			
	0.4720	0.1120			
	0.5493	0.1218			
	<0.5290>	<0.1111>			
25	0.9176	0.4434	71.7	90	25
	0.9601	0.4432			
	0.9543	0.3640			
	0.8344	0.3451			
	0.6681	0.3904			
	<0.8669>	<0.3972>			
15	2.2082	1.5086	54.8	70	20
	1.5101	1.0090			
	1.4709	0.8819			
	1.9315	1.4134			
	1.4571	0.7381			
	<1.7156>	<1.1102>			
10	5.4217	3.8619	41.8	90	33
	3.3201	2.5364			
	3.0545	2.6963			
	3.1689	2.3505			
	6.5457	4.7413			
	<4.3022>	<3.2373>			
7.5	9.8526	6.1483	42.4	70	18
	7.2672	5.8472			
	6.5794	5.1530			
	7.1989	5.7303			
	6.8079	5.3798			
	<7.5412>	<5.6517>			
5	70.289	65.427	37.7	40	45
	20.509	14.450			
	16.376	11.239			
	42.223	36.034			
	16.120	13.139			
	<33.103>	<28.058>			
2.5	61.438	51.940	7.4	10	80
	65.974	65.974			

72.243	72.243
68.145	68.145
95.039	94.821
<72.568>	<70.625>

Table S6. Quality and accuracy of fits to synthetic RESPDOR data for (*dm*Phebox)Ir/Al₂O₃ (90:10).

S/N	1-structure χ^2	2-structure χ^2	CL / %	structure accuracy / %	population deviation / %
100	0.2250	0.0343	98.9	100	0
	0.2117	0.0243			
	0.2309	0.0209			
	0.2312	0.0350			
	0.2212	0.0287			
	<0.2240>	<0.0286>			
50	0.3451	0.1266	83.5	100	0
	0.2834	0.0920			
	0.3406	0.1261			
	0.2643	0.0847			
	0.3725	0.1205			
	<0.3212>	<0.1100>			
25	0.5683	0.4074	44.3	100	2
	0.7833	0.6081			
	0.6862	0.4805			
	0.7020	0.5487			
	0.6677	0.4930			
	<0.6815>	<0.5075>			
15	1.7087	1.3952	44.3	60	35
	2.4268	1.8135			
	1.7863	1.4799			
	1.9779	1.2555			
	1.9104	1.2960			
	<1.9620>	<1.4480>			
10	2.9864	2.7973	28.1	60	22
	3.2142	2.8975			
	3.1500	2.6003			
	2.1058	1.9868			
	2.8833	2.2813			
	<2.8680>	<2.5126>			
7.5	6.5729	5.1628	40.1	50	24
	7.2546	6.8765			
	7.7675	6.1976			
	11.046	6.7431			
	12.579	9.1281			
	<9.0443>	<6.8216>			
5	24.944	18.697	25.3	30	53
	44.059	43.342			
	22.651	20.685			
	55.876	53.355			
	37.508	32.291			
	<37.008>	<33.674>			

2.5	73.025	72.992	5.6	0	100
	63.613	63.585			
	93.356	92.462			
	68.439	66.958			
	94.803	94.450			
	<78.647>	<78.089>			

Table S7. Quality and accuracy of fits to synthetic RESPDOR data for (*dm*Phebox)Ir/Al₂O₃ (100:0).

S/N	1-structure χ^2	2-structure χ^2	CL / %	structure accuracy / %	population deviation / %
100	0.0519	0.0292	55.4	100	0
	0.0401	0.0275			
	0.0410	0.0254			
	0.0296	0.0202			
	0.0411	0.0252			
	<0.0407>	<0.0255>			
50	0.1086	0.0910	29.8	100	0
	0.1066	0.0898			
	0.1124	0.1038			
	0.1191	0.1077			
	0.1320	0.1111			
	<0.1157>	<0.1007>			
25	0.3851	0.3816	24.4	100	8
	0.4555	0.3941			
	0.5277	0.4720			
	0.4577	0.3679			
	0.3385	0.3206			
	<0.4329>	<0.3872>			
15	0.7932	0.7499	24.2	100	6
	1.1106	0.8668			
	1.2103	1.1452			
	1.3944	1.2721			
	1.2553	1.1912			
	<1.1528>	<1.0450>			
10	7.5224	6.5717	31.2	80	54
	4.1472	3.7082			
	6.0567	4.5653			
	3.0795	2.8734			
	3.7554	3.1109			
	<4.9122>	<4.1659>			
7.5	50.168	46.281	31.0	80	56
	19.955	18.202			
	5.0849	4.5628			
	11.455	9.4050			
	14.252	9.6715			
	<20.183>	<17.624>			
5	48.373	48.013	23.1	60	84
	19.257	17.070			
	17.028	12.627			
	10.289	9.4871			

	77.766	75.734			
	<34.543>	<32.586>			
2.5	80.990	80.939	4.5	0	100
	135.21	135.21			
	122.61	121.22			
	84.268	84.250			
	69.338	68.128			
	<98.484>	<97.951>			

Table S8. Quality and accuracy of fits to synthetic REDOR data for (NHC)Pt/SiO₂.

S/N	1-structure χ^2	2-structure χ^2	CL / %	structure accuracy / %	population deviation / %
100	2.3934	0.4366	98.5	90	4
	2.3044	0.2781			
	2.3180	0.3150			
	2.2992	0.3058			
	2.2290	0.3065			
	<2.3088>	<0.3284>			
50	2.6828	0.5640	95.0	70	8
	2.5048	0.4876			
	2.6210	0.5813			
	2.5426	0.4914			
	2.6230	0.5528			
	<2.5949>	<0.5354>			
25	3.0282	1.2198	79.3	90	16
	3.1892	1.2936			
	3.0061	1.2051			
	3.1647	1.2440			
	3.1727	1.0278			
	<3.1122>	<1.1981>			
15	5.7079	3.6794	63.3	80	20
	4.9661	2.6840			
	5.5532	2.6700			
	4.9033	2.2866			
	4.5925	2.8722			
	<5.1446>	<2.8385>			
10	16.4127	13.715	42.1	40	48
	10.5241	7.0600			
	26.2491	23.084			
	16.5870	12.287			
	9.12321	6.1458			
	<15.7792>	<12.458>			
7.5	44.0441	36.539	34.0	60	76
	38.8287	33.751			
	20.1957	16.175			
	25.6586	22.376			
	20.8328	16.923			
	<29.9120>	<25.153>			
5	84.2597	81.831	13.6	50	72
	87.2260	82.938			
	79.2405	75.898			

	2866.90	2851.8			
	121.847	118.10			
	<647.895>	<642.13>			
2.5	659.583	654.81	6.9	40	92
	1397.41	1390.3			
	1505.08	1484.8			
	997.414	972.55			
	120990	120990			
	<25109.9>	<25098.5>			

Table S9. Quality and accuracy of fits to synthetic REDOR data for (Phen)Zn/SiO₂.

S/N	1-structure χ^2	2-structure χ^2	CL / %	structure accuracy / %	population deviation / %
100	1.3511	0.0487	100.0	100	0
	1.4130	0.0527			
	1.4670	0.0432			
	1.2363	0.0380			
	1.2953	0.0440			
	<1.3525>	<0.0453>			
50	1.6504	0.2186	99.4	100	0
	1.5786	0.1457			
	1.5211	0.1911			
	1.6649	0.1823			
	1.4615	0.1737			
	<1.5753>	<0.1823>			
25	1.7902	0.6117	84.9	60	20
	1.8745	0.6061			
	2.3480	0.6044			
	2.3169	0.7260			
	2.2575	0.8899			
	<2.1174>	<0.6876>			
15	2.9488	1.7172	60.8	70	16
	2.4493	1.3417			
	3.1950	1.8343			
	2.9005	1.6176			
	3.0297	1.8878			
	<2.9047>	<1.6797>			
10	6.6166	4.6266	48.9	70	36
	7.1705	5.4280			
	14.737	8.7608			
	5.2393	3.6565			
	4.3898	3.2364			
	<7.6308>	<5.1416>			
7.5	29.046	27.426	34.2	80	40
	11.238	8.4850			
	17.111	13.224			
	66.990	64.098			
	9.9752	6.7959			
	<26.872>	<24.006>			
5	384.69	373.42	21.3	50	72
	72.435	70.329			

	26.895	21.579			
	53.086	41.150			
	422.26	422.26			
	<191.87>	<185.75>			
2.5	3666.4	3638.6	4.2	50	96
	1550.6	1550.5			
	3672.4	3672.4			
	95.790	93.040			
	342450	342450			
	<70287>	<70280>			

Table S10. Quality and accuracy of fits to synthetic REDOR data for $(\kappa^2\text{-(NiPr)}_2\text{CH})_2\text{Sc/SiO}_2$.

S/N	1-structure χ^2	2-structure χ^2	CL / %	structure accuracy / %	population deviation / %
100	0.1373	0.0738	65.9	50	24
	0.1518	0.0746			
	0.1275	0.0740			
	0.1361	0.0697			
	0.1514	0.0756			
	<0.1408>	<0.0735>			
50	0.1832	0.1157	53.7	50	20
	0.1870	0.1242			
	0.1987	0.1104			
	0.1516	0.1159			
	0.1516	0.0953			
	<0.1744>	<0.1123>			
25	0.4003	0.3181	32.2	50	20
	0.4258	0.3891			
	0.3055	0.2543			
	0.3775	0.3655			
	0.2870	0.1997			
	<0.3592>	<0.3053>			
15	0.8350	0.8151	19.4	60	44
	0.6635	0.6081			
	0.8273	0.8229			
	0.7404	0.6707			
	0.7468	0.6526			
	<0.7626>	<0.7139>			
10	2.9294	2.8854	13.0	50	64
	1.0710	1.0230			
	4.1769	4.0408			
	2.5877	2.5512			
	2.4380	2.3656			
	<2.6406>	<2.5732>			
7.5	12.603	12.084	14.0	50	56
	5.0274	4.7939			
	22.875	22.779			
	4.7082	4.6621			
	6.9108	6.3623			
	<10.425>	<10.136>			
5	12.881	12.285	4.2	50	100

	59.153	59.153			
	29.081	29.081			
	62984	62864			
	27421	274218			
	<18101>	<18077>			
2.5	647.02	647.02	0.0	50	100
	556.26	556.26			
	3735.1	3735.1			
	164.45	164.45			
	174.29	174.29			
	<1055.4>	<1055.4>			

Supplementary References

- (1) R. Wischert, P. Laurent, C. Copéret, F. Delbecq, P. Sautet, *J. Am. Chem. Soc.* 2012, **134**, 14430–14449.
- (2) S. R. Flynn, O. J. Metters, I. Manners, D. F. Wass, *Organometallics* 2016, **35**, 847–850.